Engineering Supramolecular Polymer Conformation for Efficient Carbon Nanotube Sorting

*Theodore Z. Gao, Zehao Sun, Xuzhou Yan, Hung-Chin Wu, Hongping Yan, and Zhenan Bao**

Supramolecular polymer sorting is a promising approach to separating single-walled carbon nanotubes (CNTs) by electronic type. Unlike conjugated polymers, they can be easily removed from the CNTs after sorting by breaking the supramolecular bonds, allowing for isolation of electronically pristine CNTs as well as facile recycling of the sorting polymer. However, little is understood about how supramolecular polymer properties affect CNT sorting. Herein, chain stoppers are used to engineer the conformation of a supramolecular sorting polymer, thereby elucidating the relationship between sorting efficacy and polymer conformation. Through NMR and UV–vis spectroscopy, small-angle X-ray scattering (SAXS), and thermodynamic modeling, it is shown that this supramolecular polymer exhibits ring–chain equilibrium, and that this equilibrium can be skewed toward chains by the addition of chain stoppers. Furthermore, by controlling the stopper–monomer ratio, the sorting yield can be doubled from 7% to 14% without compromising the semiconducting purity (>99%) or properties of sorted CNTs.

1. Introduction

Single-walled carbon nanotubes (CNTs) are a promising candidate for flexible and stretchable electronics, offering exceptional electrical properties as well as mechanical robustness.[1–7] However, CNTs are typically produced as a mixture of semiconducting and metallic species, whereas most applications require CNTs of a single electronic type. To address this issue, many different purification methods have been investigated in recent years. Of particular note is polymer sorting, which has demonstrated yields of >20%, processing times within an hour, and semiconducting purities of >99.99%.[8–11] Despite significant progress in sorting efficacy, a remaining bottleneck is the cost of the sorting polymer itself. Commonly used sorting polymers cost hundreds to thousands of dollars per gram, while unsorted CNTs can be purchased for tens of dollars per gram.[11,12] Developing sorting polymers that can be removed from sorted CNTs and subsequently recycled is therefore critical to realizing low-cost CNT purification. Moreover, removal of the polymer from sorted CNTs is necessary for attaining superlative device performance, as the presence of excess sorting polymer in CNT electronics is known to degrade important device metrics such as current density, on–off ratio, and charge carrier mobility, among others.[13–16]

Thus far, development of sorting polymers has focused on covalently bonded systems, specifically conjugated polymers. Though several recyclable conjugated polymers have been reported,[17–22] these polymers cannot be recycled indefinitely as they are known to undergo scission during ultrasonication,[23,24] a key step of the sorting process. Furthermore, many of these approaches rely on triggered degradation, and therefore require resynthesis between sorting cycles. In contrast, supramolecular polymers that exhibit reversible bonding can be recycled indefinitely without resynthesis.[25–28] However, the relationship between supramolecular polymer properties and CNT sorting efficacy is poorly understood, precluding the development of an efficient and scalable CNT sorting platform based on supramolecular polymers.

To gain insight into how supramolecular polymers sort CNTs, we utilize chain stoppers, which are known to be an effective way of controlling the degree of polymerization and conformation of supramolecular polymers (**Figure 1**).[29–35] The specific system we use is a hydrogen-bonding polymer incorporating 2-ureido-4-pyrimidone (UPy).[27] The monomer consists of a fluorene moiety, which is known to be selective for semiconducting CNTs,[8–11] flanked by two UPy units that

T. Z. Gao
Department of Materials Science & Engineering
Stanford University
Stanford, CA 94305, USA
Z. Sun,[+] Dr. X. Yan,[++] Dr. H.-C. Wu, Dr. H. Yan, Dr. Z. Bao
Department of Chemical Engineering
Stanford University
Stanford, CA 94305, USA
E-mail: zbao@stanford.edu
Z. Sun
College of Chemistry and Molecular Engineering
Peking University
Beijing 100871, P. R. China
The ORCID identification number(s) for the author(s) of this article can be found under https://doi.org/10.1002/smll.202000923.
[+]Present address: Department of Materials Science and Engineering, MIT, Cambridge, MA 02139, USA
[++]Present address: School of Chemistry and Chemical Engineering, Shanghai Jiao Tong University, Shanghai 200240, P. R. China

DOI: 10.1002/smll.202000923

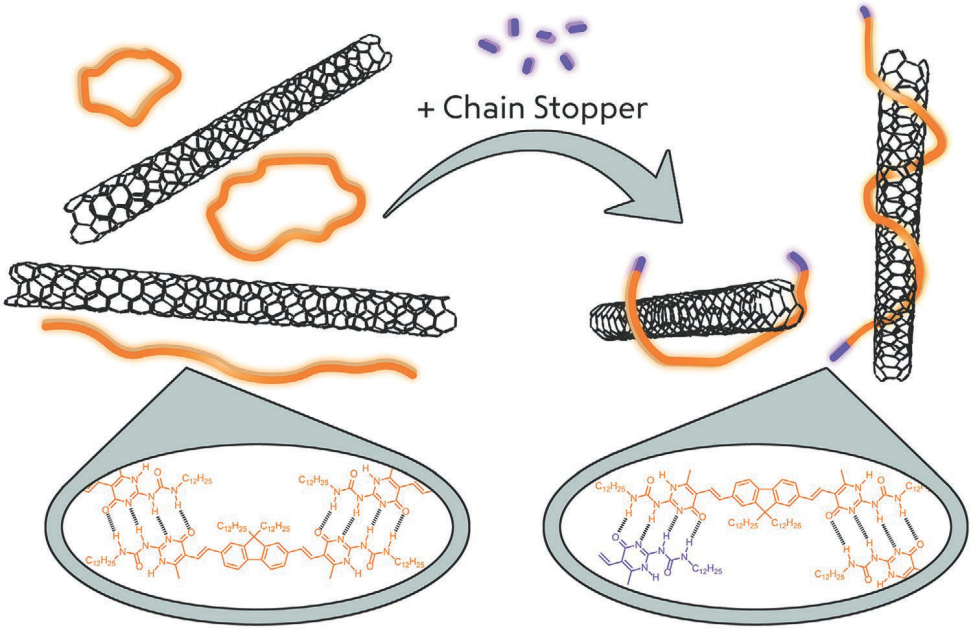

Figure 1. Schematic illustration of tuning supramolecular polymer conformation via chain stoppers. Orange denotes the supramolecular polymer, while purple denotes the chain stopper.

enable reversible H-bonding. The stopper consists of a monofunctional UPy unit that can bind to the monomer, thereby preventing it from self-associating. We previously showed that this supramolecular polymer possesses excellent sorting yield (≈10%) and semiconducting purity (>99%), in addition to having the ability to sort CNTs of a wide range of diameters (0.7–2.2 nm).[28] These characteristics make this supramolecular polymer a promising system for studying the relationship between supramolecular polymer properties and CNT sorting efficacy.

Herein, we report that this supramolecular polymer exhibits ring–chain equilibrium, a characteristic previously observed for other supramolecular polymers (**Figure 2**a). We also show that this equilibrium—and by extension, polymer conformation—can be tuned by the amount of chain stoppers added. Moreover, we find that controlling the stopper–monomer ratio can double the sorting yield from 7% to 14% without compromising the semiconducting purity (>99%) or properties of sorted CNTs.

2. Results and Discussion

2.1. Ring–Chain Equilibrium

The existence of ring–chain equilibrium in UPy-based systems is well established, though the proportion of rings and chains can depend on various factors, such as monomer length, monomer rigidity, and π–π stacking.[36–40] If present, however, it can have a significant effect on the degree of polymerization and polymer conformation, which are both known to affect CNT sorting yield and selectivity.[41–44] We therefore first set out to determine whether the supramolecular polymer exhibits ring–chain equilibrium.

To evaluate the size of the supramolecular polymer in solution, we utilized diffusion-ordered NMR spectroscopy (DOSY). This method is capable of measuring the diffusion coefficients of species in solution, which are inversely related to their hydrodynamic radii.[45] DOSY was performed on samples of the supramolecular polymer dispersed in $CDCl_3$, and the diffusion coefficient as a function of monomer concentration was extracted using the Stejskal–Tanner equation (Figure 2b).[46] Two distinct regimes can be seen, with a transition at $c \cong 10 \times 10^{-3}$ M. This trend matches observations of ring–chain equilibrium in other supramolecular systems, where there is a critical concentration below which a ring-like conformation is dominant, and above which rings and chains are both present.[36–40]

To gain further insight into these two regimes, we performed a Bayesian transformation[47] of the DOSY data, a technique that visualizes the distribution of diffusion coefficients in a multispecies system. For a sample with $c \cong 5 \times 10^{-3}$ M, only a single peak is visible, indicating that only one species is present (Figure S1a, Supporting Information). On the other hand, for a sample with $c \cong 15 \times 10^{-3}$ M, a bimodal distribution is observed, suggesting the coexistence of two species of different sizes (Figure S1b, Supporting Information). These results are in good agreement with the literature on ring–chain equilibrium, wherein chains can only exist at concentrations above the critical concentration.[36–40] Moreover, the peaks are narrow for both samples, suggesting that the distribution of sizes for both species is small. The remainder of our analysis therefore assumes a narrow distribution of molecular weights for both rings and chains.

Ring–chain equilibria in supramolecular systems can also be predicted using thermodynamic models as recently demonstrated by Meijer and co-workers.[48,49] The model is predicated on mass balance—the total concentration of the supramolecular monomer is equal to the sum of the

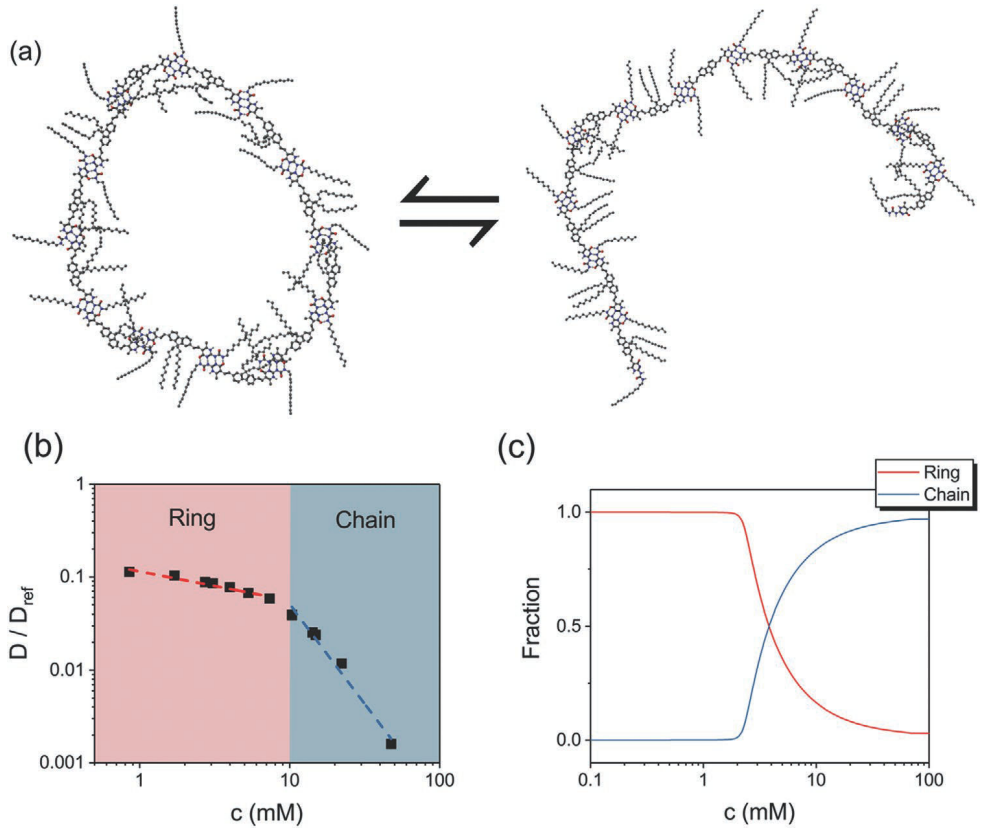

Figure 2. a) Schematic illustration of ring–chain equilibrium of the UPy-based supramolecular polymer. b) Measured diffusion constants as a function of monomer concentration. A transition in size-concentration scaling indicative of ring–chain equilibrium can be observed around $c = 10 \times 10^{-3}$ M. All values are normalized to the diffusion constant of tetramethylsilane (TMS). c) Modeled ring and chain fractions as a function of monomer concentration ($K = 6 \times 10^{-7}$ M^{-1}, $EM_1 = 1 \times 10^{-3}$ M). Ring and chain fractions are equivalent at $c = 2.5 \times 10^{-3}$ M, which represents the modeled critical concentration.

ring and chain populations, which are in turn related to various parameters such as the coupling constant, effective molarity, and the fractional extent of polymerization. We adapted their model for our system in chloroform, using a coupling constant of $K = 6 \times 10^{-7}$ M^{-1}, which is the measured coupling constant of UPy in chloroform.[50] Due to the rigid and conjugated backbone of the monomer, we assumed that rings of the supramolecular polymer are strained. The presence of ring strain is known to significantly affect the effective molarity of the monomeric ring (EM_1), one of the input parameters for the model.[35,51] Due to the lack of distinct ^{1}H NMR peaks for rings and chains of our supramolecular polymer, we were not able to extract this parameter from our experimental data. We therefore chose to use $EM_1 = 1 \times 10^{-3}$ M, the value Meijer and co-workers utilized for strained, UPy-based rings.[48] The model predicts that the fraction of rings and chains are equivalent at $c \cong 2.5 \times 10^{-3}$ M in chloroform (Figure 2c), which differs from our experimental finding that the critical concentration occurs at $c \cong 10 \times 10^{-3}$ M. This difference may be due to our assumptions regarding both the coupling constant as well as EM_1, as these values were measured for disparate UPy-based systems. The dependence of the calculated critical concentration on EM_1 is illustrated in Figure S2 (Supporting Information), showing order-of-magnitude agreement with our experimental results for a wide range of EM_1 values.

2.2. Controlling Polymer Conformation via Chain Stoppers

Having determined that the supramolecular polymer exhibits ring–chain equilibrium, we then investigated the effect of chain stoppers on polymer conformation. First we compared the transformed DOSY spectra of two samples with and without stopper (**Figure 3**a; Figure S1b, Supporting Information). A high monomer concentration, $c \cong 15 \times 10^{-3}$ M, was used to ensure that chains would be present. Figure S1b (Supporting Information) contains a bimodal distribution along the diffusion axis, confirming the coexistence of rings and chains. Figure 3a, on the other hand, reveals three distinct peaks along the diffusion axis, labeled as yellow, blue, and red in order of highest to lowest diffusion coefficient. The blue and yellow species exhibit ^{1}H resonances around 6 ppm, as well as a peak at 2.32 ppm, corresponding to an aryl methyl proton. Both of these resonances are characteristic of the stopper.[27] This suggests that the red species does not contain the stopper molecule and can therefore be attributed to rings of the supramolecular polymer. Contrarily, the blue and yellow species must contain the stopper

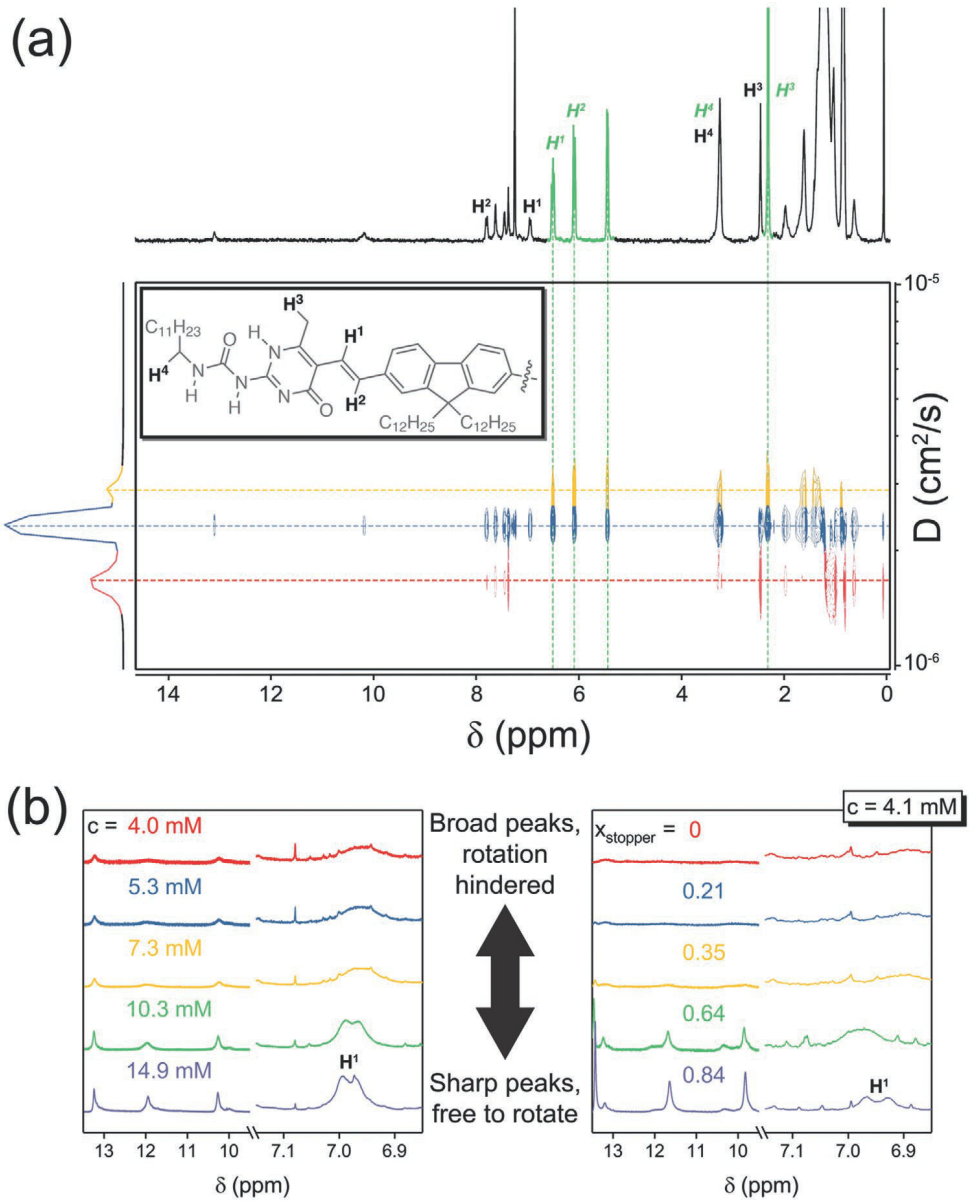

Figure 3. Controlling polymer conformation via chain stoppers. a) Bayesian transform of DOSY data for $c = 14.9 \times 10^{-3}$ M and $x_{stopper} = 0.72$. Inset—partial chemical structure of the monomer. The diffusion constant (D) is plotted along the vertical axis, while ^{1}H chemical shifts are plotted along the horizontal axis. The trace left of the plot is the integrated sum of ^{1}H signals from all protons as a function of D, and shows three distinct peaks (red, blue, yellow), suggesting the coexistence of rings, chains, and stopper dimers. The trace above the plot is the ^{1}H NMR spectra of the sample, with peaks labeled according to the inset. The monomer peaks are labeled in black, while the corresponding hydrogens from the stopper are labeled in green italics. b) ^{1}H NMR of the supramolecular polymer at different concentrations (left) and $c = 4.1 \times 10^{-3}$ M with different stopper mole fractions (right). The peak labeled as H^1 sharpens and splits as the monomer or stopper concentration is increased, indicative of conformational exchange. Peaks here and elsewhere in the text are labeled according to the inset in panel (a).

molecule. The yellow species, however, does not contain any of the ^{1}H resonances associated with the monomer, leading us to believe that the yellow species are stopper dimers formed by excess, unbound stopper molecules. This hypothesis is further supported by the fact that the yellow species has the highest diffusion coefficient, while the species containing signals from the monomer (red and blue) diffuse much slower.[30] Since the blue species contains signals from both the monomer and the stopper, we conclude that it represents chains endcapped by the stopper. These findings indicate that the stopper is indeed capable of capping chains of the supramolecular polymer, and that the presence of stopper leads to the coexistence of rings, chains, and stopper dimers.

To determine whether the size of the supramolecular polymer is affected by the stopper–monomer ratio, we performed DOSY on a sample with a lower mole fraction of stopper ($x_{stopper} = 0.17$ instead of 0.72; Figure S1c, Supporting Information). $x_{stopper}$ is defined in Equation (1)

$$x_{\text{stopper}} = \frac{[\text{stopper}]}{[\text{stopper}] + [\text{monomer}]} \quad (1)$$

Like in Figure 3a, ^{1}H resonances characteristic of the monomer and stopper can be observed for one of the species—in this case, the red species—suggesting that the red species are chains capped by stopper. The blue species does not contain these resonances, and thus constitutes rings of the supramolecular polymer. We note that the chains are the slowest diffusing species at $x_{\text{stopper}} = 0.17$, while rings are the slowest diffusing species at $x_{\text{stopper}} = 0.72$. As the stopper is unlikely to affect the size of rings, this indicates that the addition of stopper also decreases the degree of polymerization of chains, as expected for supramolecular systems.[30,33,34]

To study the relationship between polymer conformation and temperature, we performed variable-temperature (VT) NMR. A low monomer concentration of $c = 4.1 \times 10^{-3}$ M was selected so that the dominant conformation would be rings at room temperature. For temperatures near room temperature, the peak of the olefin proton at 7 ppm is broad, but as temperature is increased or decreased, the peak sharpens (Figure S3, Supporting Information). Based on our DOSY results, this phenomenon can potentially be attributed to conformational exchange. Utilizing heteronuclear multiple bond correlation (HMBC) analysis, we assigned the ^{1}H resonance at 7 ppm to the atom labeled H^1 rather than H^2 (Figure S4, Supporting Information). This suggests that as temperature is changed, the rotation of bond A is either facilitated (increasing temperature) or frozen out (decreasing temperature). This in turn changes the timescale of conformational exchange during NMR spectra acquisition, ultimately resulting in the observed peak sharpening.[52] The downfield H-bonding resonances around 12 and 13 ppm also exhibit similar sharpening at low temperatures, which we attribute to the temperature dependence of UPy coupling.

The possibility of conformational exchange is further supported by 1D ^{1}H NMR. Toward this end, we examined the NMR spectra of samples above and below the critical concentration without stopper (Figure 3b, left). When c is less than the critical concentration, the peak around 7 ppm is broad, but as c is increased, the peak sharpens, eventually forming a well-defined doublet. This implies that the conformation of the supramolecular polymer becomes less constrained as c is increased. This result qualitatively matches the concentration-dependent ring–chain equilibrium observed in DOSY. Additionally, the peak begins to sharpen at around 10×10^{-3} M, in quantitative agreement with our DOSY results.

A similar peak sharpening is seen when we add the stopper to a sample with c lower than the critical concentration (Figure 3b, right). At low stopper mole fractions, or with no stopper present, there is severe broadening of the ^{1}H peak around 7 ppm, indicating that the supramolecular polymer exists in a constrained conformation characteristic of rings. At high stopper mole fractions, the peak is sharp, suggesting that the supramolecular polymer has a flexible conformation typical of chains. Furthermore, as chains normally do not exist in dilute conditions, this demonstrates that the stopper is capable of disrupting rings of the supramolecular polymer even at concentrations below the critical concentration. Altogether, these NMR results show that the conformation distribution can be skewed toward chains by increasing temperature or by adding chain stoppers.

2.3. Validating Ring–Chain Equilibrium in Toluene

Hitherto, our characterization of the supramolecular polymer has been performed in chloroform due to its poor solubility in other common organic solvents. CNT sorting, however, is typically done in aromatic solvents like toluene, rather than polar solvents like chloroform. Previous attempts at sorting CNTs in polar solvents have led to poor selectivity.[53–55] This is often hypothesized to arise from screening of the dipole interactions of metallic CNTs by polar solvents, preventing aggregation of metallic CNTs during centrifugation.[55–58] As the solubility of the monomer in toluene was too low ($<1 \times 10^{-3}$ M) for in-depth NMR or rheology studies, we chose to use solution small-angle X-ray scattering (SAXS) to study the size of the supramolecular polymer as a function of stopper mole fraction. The SAXS spectra were fitted using a two-level unified fit in Igor Pro consisting of one Guinier contribution and two Porod contributions (Figure S5, Supporting Information).[59–61] **Figure 4**a reveals that the average radius of gyration initially increases and then decreases as stopper is added. We attribute the increase in R_g to increased aggregation—as stopper is added, rings unfold into chains, which can aggregate more easily compared to rings. The decrease in R_g is likely due to shrinking of chains. These results indicate that ring–chain equilibrium also takes place in toluene. This conclusion is further supported by thermodynamic modeling, which predicts ring–chain equilibrium with a critical concentration around 26×10^{-3} M (Figure S6, Supporting Information). This suggests that for toluene, rings are the dominant conformation at all experimentally accessible concentrations.

In addition to solution SAXS, we also probed the hyperchromic effect, which describes changes in absorbance as a function of bond dissociation. This effect is particularly well known for DNA[62] and has been observed in other supramolecular systems.[63–65] To ensure that our analysis is valid, we verified that the stopper and supramolecular polymer do not have overlapping UV–vis peaks (Figure S7, Supporting Information). We find that the absorbance of the supramolecular polymer increases linearly with stopper mole fraction up to a certain point where it plateaus (Figure 4b). Intuitively, this suggests that as the stopper is added, the supramolecular polymer strands dissociate and shorten until the solution is composed solely of trimers—a monomer bonded to two chain stoppers. In theory, when x_{stopper} is 0.66, there is exactly two stopper molecules for each monomer, which is in good agreement with our data, as the plateau begins at $x_{\text{stopper}} \cong 0.6$. The slight difference between our experimental findings and the theoretical threshold value of $x_{\text{stopper}} = 0.66$ is likely due to weighing errors, which was kept below 10% for this study.

To confirm that the supramolecular polymer is fully depolymerized at high stopper mole fractions, we investigated temperature-dependent hyperchromicity for samples with varying stopper mole fractions (Figure S8, Supporting Information). At a high stopper mole fraction, no change in absorbance is

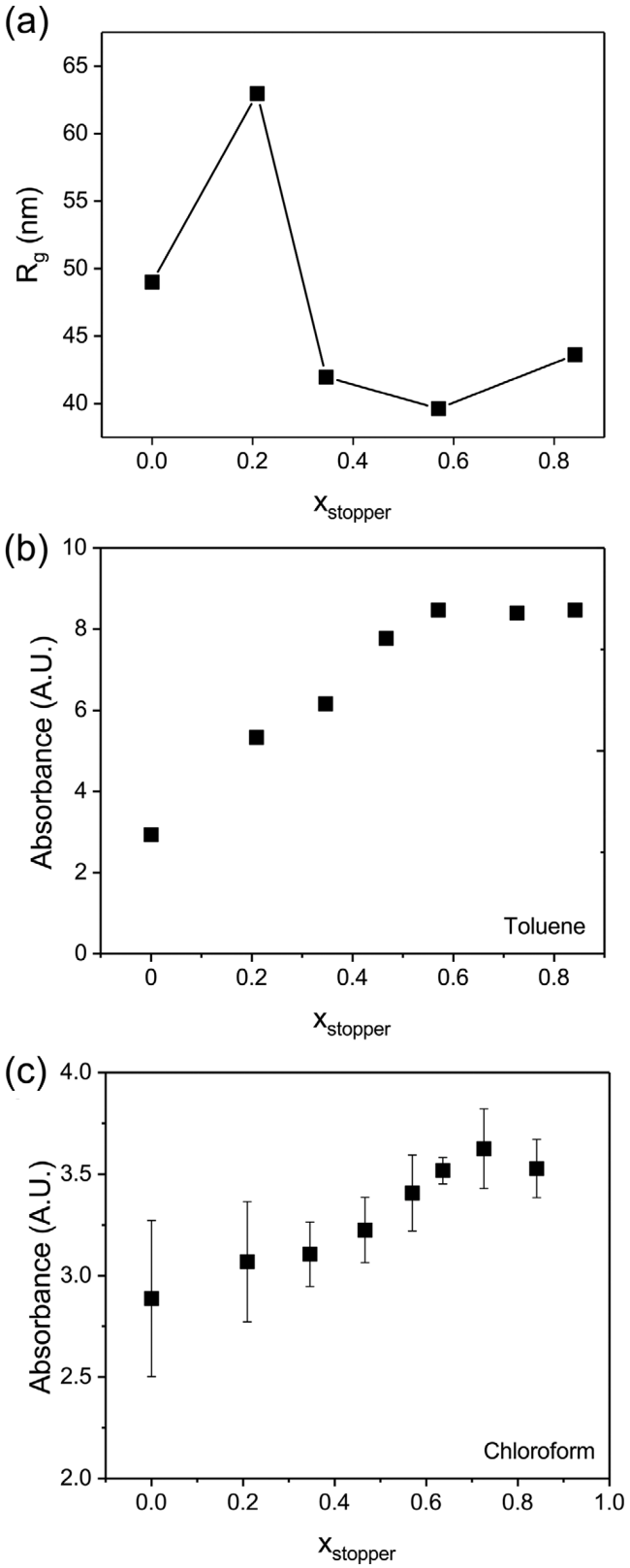

Figure 4. Validating ring–chain equilibrium in toluene ($c = 0.2 \times 10^{-3}$ M). a) Radius of gyration of the supramolecular polymer in toluene as a function of $x_{stopper}$, extracted from solution SAXS data. b,c) Absorbance of the supramolecular polymer as a function of $x_{stopper}$ in b) toluene and c) chloroform. A similar hyperchromic response can be observed in both solvents.

observed as the temperature is changed, implying that the supramolecular polymer exists in a trimeric form and cannot depolymerize further. Conversely, at low stopper mole fractions or with no stopper present, absorbance increases with temperature. This result demonstrates that the stopper can disrupt supramolecular polymerization in both solvents, despite an order of magnitude difference in the coupling constant.[50]

Finally, we also examined the hyperchromic effect in chloroform. Like Figure 4b,c shows that absorbance increases with $x_{stopper}$ up to 0.65, and plateaus afterward. This result suggests that the polymer–stopper interaction is similar in both solvents, and that the insight gained from characterizing the supramolecular polymer in chloroform may be applicable to understanding CNT sorting in toluene.

2.4. Effect of Polymer Conformation on CNT Sorting

CNT sorting was performed as described previously.[27,28] In brief, stopper and monomer ($c = 0.2 \times 10^{-3}$ M) were dissolved in 20 mL of solvent, then mixed with 5 mg of unsorted plasma torch CNTs and ultrasonicated. A slightly different stopper—with an iodide moiety rather than a vinyl group—was used for these set of experiments due to synthetic accessibility. The sorted CNT solution was collected after centrifugation, and subsequently analyzed by UV–vis to determine yield and semiconducting purity. Purity is defined by the metric φ, where a φ-value of 0.4 corresponds to a purity of 99.5%.[66]

Figure 5a shows that there is no significant change in semiconducting purity as the stopper mole fraction is increased, whereas yield first increases, then decreases. The yield at $x_{stopper} \cong 0.35$ is ≈14%, which is the highest reported yield for semiconducting CNTs sorted by supramolecular polymers.[25–28] From our NMR, SAXS, and UV–vis results, we believe that the addition of stopper causes the rings to unfold, followed by shortening of chains. The initial increase in yield can therefore be attributed to the formation of chains, as chains can effectively wrap around CNTs, while rings cannot. The ensuing decrease in yield is likely due to reduction of chain length, as very short chains are known to diminish yield.[41–43] At $x_{stopper} \cong 0.7$ there is no further change in sorting yield as a function of $x_{stopper}$, which is close to the point in Figure 4b where no further hyperchromicity can be observed. We postulate that the supramolecular polymer has been completely reduced to trimers at this value of $x_{stopper}$, and as stopper dimers are unable to sort CNTs on their own, further addition of stopper beyond this point has no effect on CNT sorting yield.

To corroborate this conclusion, we also performed CNT sorting in chloroform (Figure 5b). Though sorting in chloroform does not allow for selective purification of CNTs by electronic type, the dispersion yield—measured by integrating the CNT UV–vis absorption peaks—can be used to gauge a polymer's ability to disperse CNTs. Baseline subtraction was performed prior to integration utilizing the software package described in ref. [67]. We find that low stopper mole fractions ($x_{stopper} < 0.5$) have no effect on the integrated intensity, but at higher mole fractions, integrated intensity increases with $x_{stopper}$. Unlike our results in toluene, no decrease is seen at

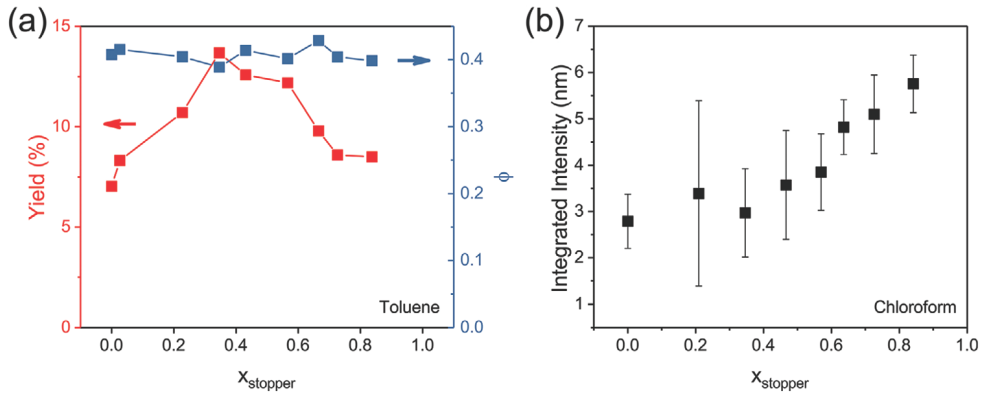

Figure 5. Effect of stopper on CNT sorting. a) Yield and semiconducting purity (φ) of CNTs sorted in toluene as a function of $x_{stopper}$, demonstrating enhanced yield at moderate values of $x_{stopper}$ without compromising purity. b) Integrated intensity of CNTs dispersed in chloroform as a function of $x_{stopper}$.

high values of $x_{stopper}$. We attribute this monotonic increase in yield to differences in the solubility of CNTs in each solvent. From a thermodynamic perspective, the free energy of solvation can be described by Equation (2)

$$\Delta G_{solvation} = \Delta G_{polymer-solvent} * f + \Delta G_{CNT-solvent} * (1-f) \quad (2)$$

where f is the fraction of the CNT surface wrapped by polymer. Figure S9 (Supporting Information) depicts the free energy of solvation for solvents with different ratios of CNT/polymer solubility. If CNT solubility is poor—as is the case for toluene—a high value of f is needed for solvation to occur. Chloroform, in contrast, has moderate CNT solubility, so the requirements for polymer wrapping are less stringent, i.e., CNT solvation can occur at lower values of f. We expect that as the stopper is added, the total number of chains in solution increases, while the average degree of polymerization decreases. CNTs are consequently solubilized by several small oligomers rather than being wrapped by a single long polymer, leading to a lower f-value. For toluene, this causes a decrease in yield at high values of $x_{stopper}$. For chloroform, however, lower f-values can still result in solvation; thus, yield increases monotonically with the total number of chains in solution, which scales with $x_{stopper}$.

Overall, these results show that CNT sorting yield can be enhanced by engineering the conformation distribution of the supramolecular sorting polymer. Moreover, these results are not unique to our choice of chain stopper, as adding small amounts of trifluoroacetic acid (TFA)—a molecule typically used to depolymerize the supramolecular polymer—yielded similar behavior (Figure S10, Supporting Information). Unlike our UPy-based stopper, however, adding high amounts of TFA undermines sorting yield and semiconducting purity due to doping.[57,58] Nevertheless, the TFA results confirm that chain stoppers and other bond disrupting agents are capable of altering the supramolecular polymer's ability to sort and disperse CNTs.

2.5. Effect of Stopper on Properties of Sorted CNTs

Lastly, we investigated CNTs sorted with different stopper mole fractions to determine whether polymer conformation has any effect on CNT properties. **Figure 6**a depicts the UV–vis spectra of CNTs sorted at various stopper mole fractions. All the spectra overlap quite well, indicating no change in chiral distribution. Figure 6b shows atomic force microscopy (AFM) length histograms of sorted CNTs, with no significant differences between them.

To test the electrical properties of these CNTs, we fabricated transistors as described previously.[15] Figure 6c shows the field-effect mobility, which does not change with the stopper mole fraction. These results demonstrate that stopper can be used to enhance sorting yield without adversely affecting the properties of sorted CNTs.

3. Conclusion

In summary, we utilized chain stoppers to control the conformation and degree of polymerization of a supramolecular polymer to improve semiconducting CNT sorting. Using NMR spectroscopy and modeling, we determined that this supramolecular polymer exhibits ring–chain equilibrium in chloroform and that the conformation distribution can be moderated by chain stoppers. Using SAXS and UV–vis spectroscopy, we found that ring–chain equilibrium also occurs in toluene, the solvent used for CNT sorting. We demonstrated that the addition of stopper allows for the sorting yield to be doubled from 7% to 14% without compromising the semiconducting purity (>99%) or properties of sorted CNTs. The approach outlined here is useful for future design of supramolecular polymer–CNT systems and may pave the way for a scalable CNT-sorting platform based on recyclable supramolecular polymers.

4. Experimental Section

Thermodynamic Modeling: The population of rings and chains were calculated using the model described in refs. [48] and [49]. Equation (3) was solved numerically for x, which was then used to determine the ring and chain populations via Equations (4) and (5)

$$c_{monomer} = EM_1 \sum_{n=1}^{\infty} n^{-3/2} x^n + \frac{x}{K(1-x)^2} \quad (3)$$

$$[R_n] = EM_1 n^{-5/2} x^n \quad (4)$$

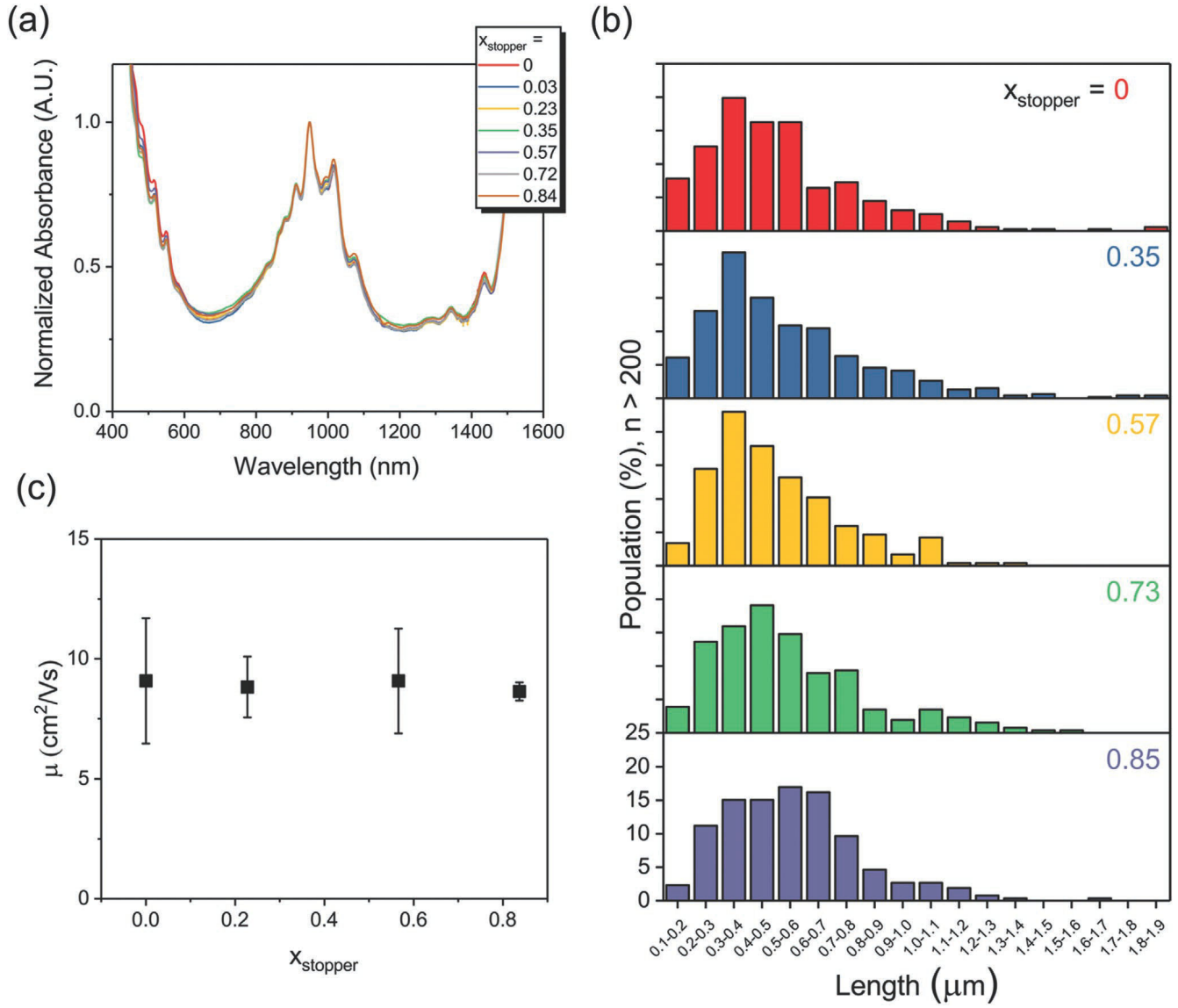

Figure 6. Effect of stopper on properties of sorted CNTs. a) UV–vis spectra of CNTs sorted at different values of $x_{stopper}$. No change in the chiral distribution can be observed. b) Length histograms of CNTs sorted at different values of $x_{stopper}$, showing no significant change in length distribution. c) Mobility of field-effect transistors made with CNTs sorted at different values of $x_{stopper}$, again showing no significant change upon adding stopper.

$$[C_n] = \frac{x^n}{K} \quad (5)$$

where x is the fractional extent of reaction, K is the UPy coupling constant, EM_1 is the effective molarity of the monomeric ring, $[R_n]$ is the concentration of rings of size n, and $[C_n]$ is the concentration of chains of size n. The model inputs were $K = 6 \times 10^{-7}$ M^{-1} (chloroform), $K = 6 \times 10^{-8}$ M^{-1} (toluene), and $EM_1 = 1 \times 10^{-3}$ M. $EM_1 = 0.1 \times 10^{-3}$ M and $EM_1 = 10 \times 10^{-3}$ M were also used to produce Figure S2 (Supporting Information).

Supramolecular Polymer Characterization: The supramolecular monomer and the chain stopper were synthesized according to the procedures in ref. [27]. Solutions of the supramolecular polymer were prepared for characterization by tip sonication (Cole-Parmer 750-Watt Ultrasonicator) or mechanical shaking. NMR spectroscopy and DOSY were performed in $CDCl_3$ using a Varian Mercury 400 MHz NMR spectrometer and a Varian Inova 600 MHz NMR spectrometer, respectively. All spectra were acquired at room temperature apart from the VT NMR spectra in Figure S3 (Supporting Information). Bayesian transformations of the DOSY data were obtained using MestReNova. Solution SAXS measurements were carried out using beamline 4-2 at SLAC National Accelerator Laboratory and fit with a two-level unified fit in Igor Pro. UV–vis measurements were done using a Cary 6000i spectrophotometer.

CNT Sorting: About 5 mg of the supramolecular monomer was dissolved in 20 mL of solvent (either toluene or chloroform) by tip sonication. The chain stopper was also added in this step for certain samples. About 5 mg of plasma torch CNTs (Raymor Industries Inc., RN-020) was then added to this dispersion and tip sonicated for 30 min at 0 °C. The resulting dispersion was subsequently centrifuged twice, once at 8000 rpm for 5 min and then at 17 000 rpm for 20 min (Sorvall LYNX 4000). The pellet was discarded in both steps, and the supernatant from the second centrifuge step was collected for further analysis.

CNT Characterization: Sorting yield was estimated from UV–vis spectra using Beer's law and assuming a 1:2 ratio of metallic to semiconducting CNTs in the unsorted material. An absorption coefficient of 35.3 mL mg^{-1} cm^{-1} was used for all calculations.[12] Semiconducting

purity was calculated by the metric φ, introduced in ref. [66], wherein a φ-value of 0.4 corresponds to a purity of 99.5%. CNT lengths were measured via tapping mode AFM (Veeco). Random-network CNT transistors with a channel length of 50 µm were fabricated on SiO_2 with Cr/Pd contacts as previously reported.[15] Field-effect mobilities were extracted from transfer characteristics measured in ambient conditions using a Keithley 4200 SCS.

Acknowledgements

T.Z.G. and Z.S. contributed equally to this work. T.Z.G. acknowledges support from the Department of Defense (DoD) through the National Defense Science & Engineering Fellowship (NDSEG) Program. Z.S. acknowledges support from the Stanford School of Engineering through the Chinese Undergraduate Visiting Researcher (UGVR) Program. Part of this work was performed at the Stanford Nano Shared Facilities (SNSF), supported by the National Science Foundation under award ECCS-1542152. SAXS measurements were carried out at the Stanford Synchrotron Radiation Lightsource, SLAC National Accelerator Laboratory, which is supported by the U.S. Department of Energy, Office of Science, Office of Basic Energy Sciences under Contract No. DE-AC02-76SF00515. The authors would like to thank Dr. Stephen Lynch for assistance with NMR measurements and interpretation.

Conflict of Interest

A patent related to this research has been submitted (US 2016/0280548 A1) and another one has been filed.

Keywords

carbon nanotubes, chain stoppers, polymer sorting, ring–chain equilibrium, supramolecular polymers

Received: February 13, 2020
Revised: April 7, 2020
Published online: June 5, 2020

[1] D. Zhong, Z. Zhang, L.-M. Peng, *Nanotechnology* **2017**, *28*, 212001.
[2] Y. Cao, S. Cong, X. Cao, F. Wu, Q. Liu, M. R. Amer, C. Zhou, *Top. Curr. Chem.* **2017**, *375*, 75.
[3] J. Zhu, M. C. Hersam, *Adv. Mater.* **2017**, *29*, 1603895.
[4] K. Chen, W. Gao, S. Emaminejad, D. Kiriya, H. Ota, H. Y. Y. Nyein, K. Takei, A. Javey, *Adv. Mater.* **2016**, *28*, 4397.
[5] A. E. Islam, J. A. Rogers, M. A. Alam, *Adv. Mater.* **2015**, *27*, 7908.
[6] L. Cai, C. Wang, *Nanoscale Res. Lett.* **2015**, *10*, 320.
[7] G. S. Tulevski, A. D. Franklin, D. Frank, J. M. Lobez, Q. Cao, H. Park, A. Afzali, S.-J. Han, J. B. Hannon, W. Haensch, *ACS Nano* **2014**, *8*, 8730.
[8] S. Qiu, K. Wu, B. Gao, L. Li, H. Jin, Q. Li, *Adv. Mater.* **2018**, *31*, 1800750.
[9] J. Lefebvre, J. Ding, Z. Li, P. Finnie, G. Lopinski, P. R. L. Malenfant, *Acc. Chem. Res.* **2017**, *50*, 2479.
[10] H. Wang, Z. Bao, *Nano Today* **2015**, *10*, 737.
[11] T. Lei, I. Pochorovski, Z. Bao, *Acc. Chem. Res.* **2017**, *50*, 1096.
[12] T. Lei, X. Chen, G. Pitner, H.-S. P. Wong, Z. Bao, *J. Am. Chem. Soc.* **2016**, *138*, 802.
[13] X. Yu, D. Liu, L. Kang, Y. Yang, X. Zhang, Q. Lv, S. Qiu, H. Jin, Q. Song, J. Zhang, Q. Li, *ACS Appl. Mater. Interfaces* **2017**, *9*, 15719.
[14] Y. Joo, G. J. Brady, C. Kanimozhi, J. Ko, M. J. Shea, M. T. Strand, M. S. Arnold, P. Gopalan, *ACS Appl. Mater. Interfaces* **2017**, *9*, 28859.
[15] T. Z. Gao, T. Lei, F. Molina-Lopez, Z. Bao, *Small Methods* **2018**, *2*, 1800189.
[16] Z. Li, J. Ding, C. Guo, J. Lefebvre, P. R. L. Malenfant, *Adv. Funct. Mater.* **2018**, *28*, 1705568.
[17] Z. Zhang, Y. Che, R. A. Smaldone, M. Xu, B. R. Bunes, J. S. Moore, L. Zang, *J. Am. Chem. Soc.* **2010**, *132*, 14113.
[18] F. Lemasson, J. Tittmann, F. Hennrich, N. Stürzl, S. Malik, M. M. Kappes, M. Mayor, *Chem. Commun.* **2011**, *47*, 7428.
[19] W. Z. Wang, W. F. Li, X. Y. Pan, C. M. Li, L.-J. Li, Y. G. Mu, J. A. Rogers, M. B. Chan-Park, *Adv. Funct. Mater.* **2011**, *21*, 1643.
[20] S. Liang, G. Chen, Y. Zhao, *J. Mater. Chem. C* **2013**, *1*, 5477.
[21] S. Liang, Y. Zhao, A. Adronov, *J. Am. Chem. Soc.* **2014**, *136*, 970.
[22] Y. Joo, G. J. Brady, M. J. Shea, M. B. Oviedo, C. Kanimozhi, S. K. Schmitt, B. M. Wong, M. S. Arnold, P. Gopalan, *ACS Nano* **2015**, *9*, 10203.
[23] J. M. Paulusse, R. P. Sijbesma, *J. Polym. Sci., Part A: Polym. Chem.* **2006**, *44*, 5445.
[24] M. M. Caruso, D. A. Davis, Q. Shen, S. A. Odom, N. R. Sottos, S. R. White, J. S. Moore, *Chem. Rev.* **2009**, *109*, 5755.
[25] F. Toshimitsu, N. Nakashima, *Nat. Commun.* **2014**, *5*, 5041.
[26] F. Toshimitsu, N. Nakashima, *Sci. Rep.* **2015**, *5*, 18066.
[27] I. Pochorovski, H. Wang, J. I. Feldblyum, X. Zhang, A. L. Antaris, Z. Bao, *J. Am. Chem. Soc.* **2015**, *137*, 4328.
[28] A. Chortos, I. Pochorovski, P. Lin, G. Pitner, X. Yan, T. Z. Gao, J. W. F. To, T. Lei, J. W. Will, H.-S. P. Wong, Z. Bao, *ACS Nano* **2017**, *11*, 5660.
[29] G. Ercolani, L. Mandolini, P. Mencarelli, S. Roelens, *J. Am. Chem. Soc.* **1993**, *115*, 3901.
[30] R. P. Sijbesma, F. H. Beijer, L. Brunsveld, B. J. B. Folmer, J. H. K. K. Hirschberg, R. F. M. Lange, J. K. L. Lowe, E. W. Meijer, *Science* **1997**, *278*, 1601.
[31] G. Ercolani, *J. Phys. Chem. B* **1998**, *102*, 5699.
[32] P. M. Saville, E. M. Sevick, *Langmuir* **1998**, *14*, 3137.
[33] T. Pinault, C. Cannizzo, B. Andrioletti, G. Ducouret, F. Lequeux, L. Bouteiller, *Langmuir* **2009**, *25*, 8404.
[34] T. Pinault, B. Andrioletti, L. Bouteiller, *Beilstein J. Org. Chem.* **2010**, *6*, 869.
[35] M. Ciaccia, I. Tosi, L. Baldini, R. Cacciapaglia, L. Mandolini, S. Di Stefano, C. A. Hunter, *Chem. Sci.* **2015**, *6*, 144.
[36] A. Tessa ten Cate, H. Kooijman, A. L. Spek, R. P. Sijbesma, E. W. Meijer, *J. Am. Chem. Soc.* **2004**, *126*, 3801.
[37] A. Tessa ten Cate, R. P. Sijbesma, *Macromol. Rapid Commun.* **2002**, *23*, 1094.
[38] S. Li, T. Xiao, W. Xia, X. Ding, Y. Yu, J. Jiang, L. Wang, *Chem. - Eur. J.* **2011**, *17*, 10716.
[39] T. Xiao, X. Feng, S. Ye, Y. Guan, S.-L. Li, Q. Wang, Y. Ji, D. Zhu, X. Hu, C. Lin, Y. Pan, L. Wang, *Macromolecules* **2012**, *45*, 9585.
[40] H. M. Keizer, J. J. González, M. Segura, P. Prados, R. P. Sijbesma, E. W. Meijer, J. de Mendoza, *Chem. - Eur. J.* **2005**, *11*, 4602.
[41] P. Imin, F. Cheng, A. Adronov, *Polym. Chem.* **2011**, *2*, 1404.
[42] F. Jakubka, S. P. Schießl, S. Martin, J. M. Englert, F. Hauke, A. Hirsch, J. Zaumseil, *ACS Macro Lett.* **2012**, *1*, 815.
[43] N. A. Rice, A. V. Subrahmanyam, S. E. Laengert, A. Adronov, *J. Polym. Sci., Part A: Polym. Chem.* **2015**, *53*, 2510.
[44] M. J. Shea, R. D. Mehlenbacher, M. T. Zanni, M. S. Arnold, *J. Phys. Chem. Lett.* **2014**, *5*, 3742.
[45] Y. Cohen, L. Avram, L. Frish, *Angew. Chem., Int. Ed.* **2005**, *44*, 520.

[46] E. O. Stejskal, J. E. Tanner, *J. Chem. Phys.* **1965**, *42*, 288.
[47] C. Cobas, S. Sykora, Smash 2008 Conference **2008**, https://doi.org/10.3247/sl2nmr08.010.
[48] T. F. Paffen, G. Ercolani, T. F. de Greef, E. W. Meijer, *J. Am. Chem. Soc.* **2015**, *137*, 1501.
[49] T. F. Paffen, A. J. Teunissen, T. F. de Greef, E. W. Meijer, *Proc. Natl. Acad. Sci. USA* **2017**, *114*, 12882.
[50] S. H. M. Söntjens, R. P. Sijbesma, M. H. P. van Genderen, E. W. Meijer, *J. Am. Chem. Soc.* **2000**, *122*, 7487.
[51] S. Di Stefano, L. Mandolini, *Phys. Chem. Chem. Phys.* **2019**, *21*, 955.
[52] A. D. Bain, *Prog. Nucl. Magn. Reson. Spectrosc.* **2003**, *43*, 63.
[53] W. Xu, J. Zhao, L. Qian, X. Han, L. Wu, W. Wu, M. Song, L. Zhou, W. Su, C. Wang, S. Nie, Z. Cui, *Nanoscale* **2014**, *6*, 1589.
[54] J.-Y. Hwang, A. Nish, J. Doig, S. Douven, C.-W. Chen, L.-C. Chen, R. J. Nicholas, *J. Am. Chem. Soc.* **2008**, *130*, 3543.
[55] H. Wang, B. Hsieh, G. Jiménez-Osés, P. Liu, C. J. Tassone, Y. Diao, T. Lei, K. N. Houk, Z. Bao, *Small* **2015**, *11*, 126.
[56] J. Ouyang, J. Ding, J. Lefebvre, Z. Li, C. Guo, A. J. Kell, P. R. L. Malenfant, *ACS Nano* **2018**, *12*, 1910.
[57] Z. Li, J. Ding, J. Lefebvre, P. R. L. Malenfant, *ACS Omega* **2018**, *3*, 3413.
[58] J. Ding, Z. Li, J. Lefebvre, X. Du, P. R. L. Malenfant, *J. Phys. Chem. C* **2016**, *120*, 21946.
[59] J. Ilavsky, *J. Appl. Crystallogr.* **2012**, *45*, 324.
[60] G. Beaucage, *J. Appl. Crystallogr.* **1995**, *28*, 717.
[61] J. Ilavsky, P. R. Jemian, *J. Appl. Crystallogr.* **2009**, *42*, 347.
[62] M. D'Abramo, C. L. Castellazzi, M. Orozco, A. Amadei, *J. Phys. Chem. B* **2013**, *117*, 8697.
[63] H. Fenniri, P. Mathivanan, K. L. Vidale, D. M. Sherman, K. Hallenga, K. V. Wood, J. G. Stowell, *J. Am. Chem. Soc.* **2001**, *123*, 3854.
[64] S. Oliver, D. S. Thomas, M. Kavallaris, O. Vittorio, C. Boyer, *Polym. Chem.* **2016**, *7*, 2542.
[65] K. K. Kartha, N. K. Allampally, S. Yagai, R. Q. Albuquerque, G. Fernández, *Chem. - Eur. J.* **2019**, *25*, 9230.
[66] J. Ding, Z. Li, J. Lefebvre, F. Cheng, G. Dubey, S. Zou, P. Finnie, A. Hrdina, L. Scoles, G. P. Lopinski, C. T. Kingston, B. Simard, P. R. L. Malenfant, *Nanoscale* **2014**, *6*, 2328.
[67] M. Pfohl, D. D. Tune, A. Graf, J. Zaumseil, R. Krupke, B. S. Flavel, *ACS Omega* **2017**, *2*, 1163.